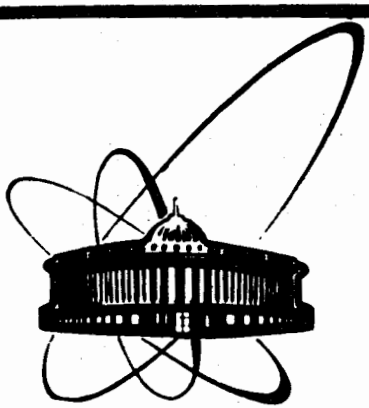

объединенный
институт
ядерных
исследований
дубна

E1-89-486

RESONANCE PATTERN OF LOW MASS MUON PAIRS PRODUCED IN 38 - GeV/c π^-C INTERACTIONS

RISK Collaboration

Submitted to International Europhysics Conference
on High Energy Physics Madrid (Spain),
september 6-13, 1989

1989

Банников А.В. и др.
E1-89-486

Резонансы как источник мюонных пар малой массы, рожденных в π^-C-взаимодействиях при 38 ГэВ/с

Представлены первые результаты эксперимента SERP-E-151, в котором изучалось рождение мюонных пар малой массы ($M_{\mu\mu} < M_{J/\psi}$) и малого поперечного импульса ($P_\perp \leq 1{,}5$ ГэВ/с) в реакции $\pi^-C \to \mu^+\mu^- + X$. Исследования проводились с помощью 5-метровой стримерной камеры с углеродными мишенями и конверторами из свинцового стекла, что позволило регистрировать полные события. Обработанный материал, содержащий ~5000 реконструированных взаимодействий с ~3300 γ-квантами, на порядок величины превышает статистику других экспериментов, регистрирующих лептонные пары вместе с γ-сопровождением. Прямое наблюдение распадов резонансов $\eta \to \mu\mu\gamma$ и $\eta' \to \mu\mu\gamma$ в спектре масс $\mu\mu\gamma$, $\rho \to \mu\mu$ и $\eta \to \mu\mu$ в спектре масс $\mu\mu$ позволяет заключить, что известные резонансы являются доминирующим источником (98±7±10)% димюонов малой массы ($0{,}2 < M_{\mu\mu} < 0{,}6$ ГэВ/с^2), рожденных в нецентральной области при $X_F \geq 0{,}4$. Этот результат не согласуется с моделью мягкой кварк-антикварковой аннигиляции.

Работа выполнена в Лаборатории ядерных проблем ОИЯИ.

Препринт Объединенного института ядерных исследований. Дубна 1989

Bannikov A.V. et al.
E1-89-486

Resonance Pattern of Low Mass Muon Pairs Produced in 38 - GeV/c π^-C Interactions

We report the first results of experiment SERP-E-151 which examined the production of muon pairs at low mass ($M_{\mu\mu} \leq M_{J/\psi}$) and low transverse momentum ($P_\perp < 1.5$ GeV/c) in the reaction $\pi^-C \to \mu^+\mu^- + X$. The measurements were carried out with a 5-meter streamer chamber with carbon targets and lead glass converters allowing the observation of the entire events. An analysed sample, consisting of ≈5000 reconstructed interactions with ≈3300 detected γ's, exceeds by an order of magnitude the statistics of other experiments detecting lepton pairs together with accompanying γ's. The direct observation of decays of resonances $\eta \to \mu\mu\gamma$ and $\eta' \to \mu\mu\gamma$ in the $\mu\mu\gamma$ - mass spectrum and $\rho \to \mu\mu$ and $\eta \to \mu\mu$ in the $\mu\mu$ - mass spectrum allows the conclusion that the known resonances represent the dominant source (98±7±10)% of low mass dimuons ($0.2 < M_{\mu\mu} < 0.6$ GeV/c^2) produced in the non - central region at $X_F \geq 0.4$. This result seems to be in disagreement with the soft quark - antiquark annihilation model.

The investigation has been performed at the Laboratory of Nuclear Problems, JINR.

Preprint of the Joint Institute for Nuclear Research. Dubna 1989

A.V.Bannikov, J.Bohm, Choe Song Hek, T.Gemesy[1],
A.K.Javrishvili[2], A.I.Kharchilava[2], N.N.Khovanskij,
Z.V.Krumstein, T.A.Lomtadze[2], Yu.P.Merekov, V.I.Petrukhin,
Gy.Pinter[2], K.Piska, K.Safarik, J.Sedlak[3], E.G.Tskhadadze[2],
G.A.Shelkov, L.S.Vertogradov, P.Zavada[3]

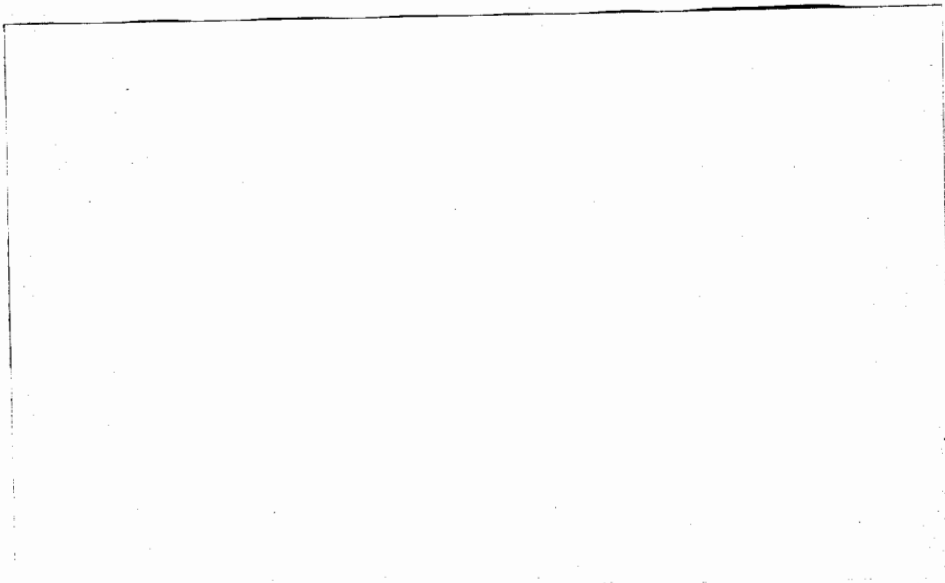

[1]Central Research Institute for Physics, Budapest, Hungary
[2]Institute of Physics, Tbilisi, GSSR
[3]Institute of Physics, Prague, Czechoslovakia

INTRODUCTION

Lepton pair production in collisions of hadrons with proton and nuclear targets has been investigated extensively in the past decade [1-17]*. A number of experiments have reported observations of anomalous dilepton production at $0.2 < M_{11} < 0.6$ GeV/c^2 and $P_\perp \leq 1$ GeV/c. Contrary to the high mass region, the production rate of low mass dilepton continuum is at least one order of magnitude larger than what would be expected from the Drell-Yan process. This excess of low mass lepton pairs over the known particle decay sources has been seen both in e^+e^- and $\mu^+\mu^-$ channels and in a wide kinematic region of x_F ($x_F = P^*_\parallel/P^*_{max}$) and $P_\perp$. However, the question about the origin of these leptons still remains open.

Bjorken and Weisberg [18] suggested that the low mass dilepton continuum might result predominantly from annihilation of quarks and antiquarks produced in the collision process. Cerny, Lichard and Pisut developed these ideas into a Monte Carlo model, the so-called soft annihilation model [19-20], and incorporated the concept of space time evolution of the collisions in order to confine the effect to low mass. The soft annihilation model has been shown to describe the data fairly well [21].

Zakharov [22] suggested the breaking of color strings as a source of low mass lepton pairs. The estimated cross section of lepton pair production with $M \sim 0.4$-0.6 GeV/c^2 and in the central region of rapidities has been brought close to the experimental data [9] by adjustment of the string tension to 0.6-0.8 GeV^2.

The observation of low mass lepton pair continuum naturally led to the question of direct real photon production. An expected value of γ/π^0-ratio deduced from lepton pair production in 10-20 GeV/c region varies from a few percent up to 10% level [4,6]. Experimental searches for real photons have isolated an excess of soft γ's over the contributions arising from hadron decays which could be attributed to hadronic inner bremsstrahlung [23] or, at higher energies, to a new fenomenon [24,25].

*Last comprehensive review is given in [17].

These protons are confined to very low x_F ($|x_F| \leq 0.01$) and small $P_\perp$ ($P_\perp \leq 0.06$ GeV/c) and clearly do not explain lepton pair anomaly if it really exists, with its broad x_F and $p_\perp$ distributions. Moreover, experiments dealing with production of e^+e^--pairs with masses less than that of the π° meson have confirmed the result obtained with the soft direct real photon searches [15,16]. It seems that there is no evidence for direct real photon and e^+e^- pair production with $M < M_{\pi^\circ}$ in the region of $x_F \geq 0.1$ and $P_\perp \leq 1$ GeV/c. Further experiments are clearly required in order to reveal the origin of some disagreement between the result obtained for real photon production and that for anomalous lepton pair production with $M=0.2 \div 0.6$ GeV/c^2.

The main goal of present experiment is the simultaneous measurement and efficient detection of muon pairs and photons allowing the reliable estimate of contributions from η, η' and ω Dalitz decays to the low mass dimuon production. Since in many respects anomalous pairs were found similar to η Dalitz pairs and about two or three times more lepton pairs than expected from η decays could explain the anomalous effect, the measurement of a direct lepton pair cross section depends crucially on the proper η background elimination. Unfortunatelly, there are no comprehensive experimental data on the η, η' and ω inclusive cross sections in the $x_F \geq 0$ region. Therefore, in previous experimental analyses, many assumptions had to be used about resonance production. It is of great importance that this experiment, for the first time, has measured η and η' contributions directly by using the $\mu\mu\gamma$ mass spectrum.

THE APPARATUS

The measurements were carried out with the RISK spectrometer of JINR at the U70 accelerator in IHEP (Serpukhov). An unseparated beam of 38 GeV/c negatively charged hadrons was focused to a 3x2 cm^2 spot at the experimental targets. Four threshold gas Cerenkov counters were placed in the beam to identify the particle type: $\pi^-:K^-:\bar{p} = 100:1.8:0.3$.

An apparatus for a detection of dimuon events is shown in Fig.1. The big magnet provided an active volume of 5.0x1.7x x1.4 m^3 and was operated at a central field of 13 kG along the vertical direction. The central device of the spectrometer was a three gap streamer chamber [26]. It was a box 4.7 m long, 0.9 m wide and 0.8 m deep with four planes of wire mesh, forming transparent electrodes. The chamber was filled with a 70% neon and 30% helium gas mixture with one part in 10^3 isobutane and also with SF_6 to keep the memory time on the 1 μsec level.

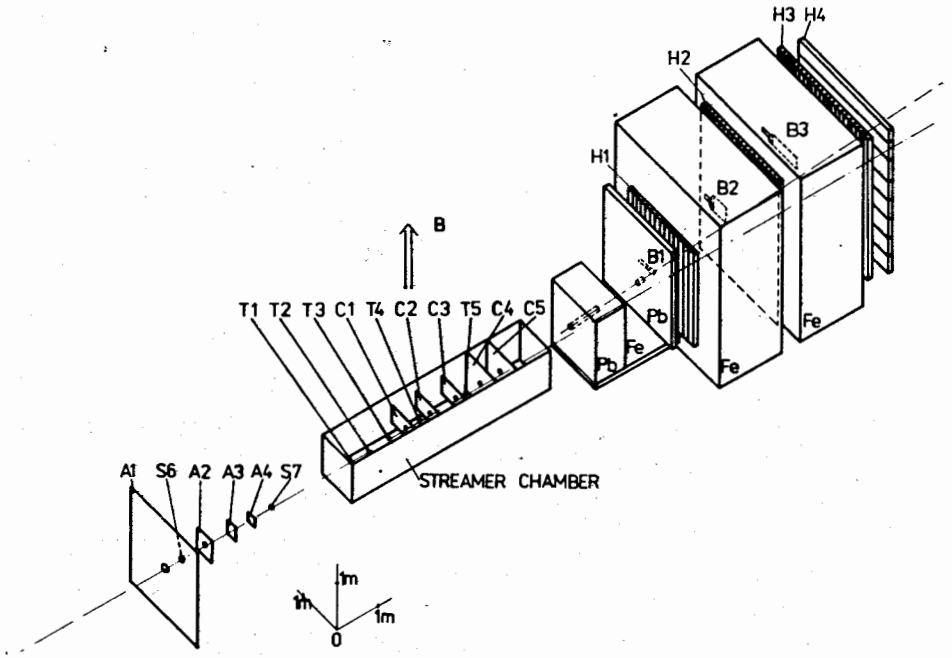

Fig.1. Layout of the experimental apparatus: A1÷A4, B1 ÷ B3 - veto counters; S6, S7 - scintillation counters of beam telescope; T1 ÷ T5 - carbon targets; C1 ÷ C5 - lead glass converters; H1 ÷H3 - vertical hodoscopes; H4 - horizontal hodoscope.

Five carbon targets were localized along the beam position in the chamber just in the 40 cm gap between the two inner electrodes. Each target was divided into two separated segments of equal thickness corresponding to 2.8% of pion interaction length and to 7.2% of radiation length in order to minimize a contamination due to secondary interactions and γ-conversions within the target. Both segments were closed into a mylar jacket 8 cm long and 8 cm in diameter, filled with freon. Final state protons of momenta less than ~0.2 GeV/c would not enter the gas of the streamer chamber and would hence be undetected.

In the chamber there were also five planes of lead glass converters with an opening ~7 cm in diameter to allow passage of the unscattered pion beam. The radiation length of lead glass used in converters was fixed to (2.0±0.1) cm. The thickness of each converter was measured in several points and, on the average, it is equal to 23% of radiation length. Details of construction and of the shielding of converters from discharges in the chamber were presented elsewhere [27].

Three vertical liquid scintillator hodoscopes H1, H2 and H3[28] and horizontal plastic scintillator hodoscope H4 were inserted in the absorber to provide trigger and tracking information. A fast processor analyzed pulses coming from the hodoscopes, the beam telescope and the veto counters and selected $\mu\mu$-candidates according to a set of trigger criteria[29]. Muons with energy less than 5.3 GeV and secondary pions were mostly absorbed in lead and iron walls of 13 interaction lengths in total thickness. The number of triggers of a streamer chamber was reduced to 1.4/pulse at the beam intensity of 1.3×10^6 particles per second. A total sample consists of 270 thousand pictures.

An off-line analysis of the tracking information has resulted in a selection of 42% of pictures for the scanning procedure. The reconstructed muon trajectory in hodoscopes provides an estimate of the coordinate and the angle of the muon track leaving the streamer chamber. Approximately, in 1/4 of the scanned pictures two tracks of particles with opposite charges satisfied the criteria, and they were measured.

There are two basic tests used in the selection of real $\mu^+\mu^-$-events. The deviations of the extrapolated measured trajectories from the real coordinates in hodoscopes H1, H2 and H3 must be less than 3σ due to multiple scattering[30], and in the target the trajectories must deviate from the vertex of the entire event by less than 3σ of the measuring errors. After this procedure, the net sample of 6536 entire $\mu^+\mu^-$-events (after the scanning of ~40% of pictures) is available for the next analysis.

To estimate the background contamination due to simultaneous $\pi^\pm \to \mu^\pm \nu$ decays remaining in the dimuon sample we have analyzed the ~7000 reconstructed π^-C events from a 2-m propane bubble chamber of LVE-JINR. The Monte Carlo simulations have shown that with the hardware, software and film processing criteria, the contamination of dimuons by background events does not exceed ~8% and it is nearly independent of the dimuon mass.

The events having the dimuon momentum $P_{\mu\mu} > 38$ GeV/c (1.8%) or the sum of momenta of all secondaries greater than 40 GeV/c (5%) have been rejected. In the subsequent analysis only the events originated in targets T3, T4 and T5 (see Fig.1) have been taken into account to decrease the background to several percent (an averaged pion decay length is 2.9 m).

RESULTS

The measured data in this experiment cover most of the region $x_F > 0$, but for the dimuon mass $M_{\mu\mu} < 0.6$ GeV/c^2 only the region $x_F > 0.4$ is available. Therefore, the cut $x_F > 0.4$ was applied to all dimuon masses and it reduces the investigated sample to 4663 events.

A scan for γ's was carried out in each picture with an identified dimuon. Nearly 3300 γ's were found by their materialization or Compton scattering in converters (89.4% of them were e^+e^- pairs). To minimize the systematic errors arising from scanning and measuring losses at low γ momenta, we imposed cutoff $P_\gamma > 50$ MeV/c. In addition, we also excluded e^+e^- pairs which had $M^2_{e^+e^-} > 0.01$ (GeV/c^2)^2 (1.8%) or did not belong to an interaction (5%). The mean value of the weighting factor accounting for detection losses is ~2.5. A gaussian fit to π° peak which is clearly visible in the invariant mass distribution of two γ's yielded the value of $\langle m_{\pi^\circ} \rangle = 125 \pm 13$ MeV/c^2 and $\sigma = 35$ MeV/c^2.

In order to elucidate the dimuon production arising from η, η' and ω Dalitz decays we investigated the invariant mass distribution of the $\mu^+\mu^-\gamma$ system. The experimental data for dimuon masses $M_{\mu\mu} < 0.6$ GeV/c^2 and $M_{\mu\mu} < 0.9$ GeV/c^2 are shown in Fig.2a and Fig.2c, respectively. One can see two pronounced peaks in Fig.2c corresponding to η and η' resonances. As a first step of an analysis, we subtracted from the experimental distribution the contribution originating in random $\gamma\mu\mu$ combinations of γ's emitted in π° decay. As a second step, we fitted the remaining mass spectrum by the following expression:

$$N_{\mu\mu\gamma} = a_{\pi^\circ} F(M_{\mu\mu\gamma}) + a_\eta G(m_\eta, \sigma_\eta) + a_{\eta'} G(m_{\eta'}, \sigma_{\eta'}) + a_\omega E(M_{\mu\mu\gamma}).$$

Here, $G(m,\sigma)$ denotes the Gauss distribution with mass m and measuring error σ as free parameters. The typical fitted values of measuring errors characterizing a width of the η and η' mass peaks were $\sigma_\eta \sim \sigma_{\eta'} \sim 0.11$ GeV/c^2. F and E stand for the evaluated mass distribution having rise in $\pi^\circ \to \gamma\gamma$ and $\omega \to \mu\mu\pi^\circ$ decays, respectively, and a_{π°, a_η, $a_{\eta'}$ and a_ω are the free parameters. The results of the fitting procedure are demonstrated by full lines in Figures 2b and 2d and the fitted values of the free parameters are summarized in Table 1. There are also shown the fitted yields of resonances, N_η, $N_{\eta'}$ and N_ω in two overlapping mass regions: $M_{\mu\mu} < 0.6$ GeV/c^2 and $M_{\mu\mu} < 0.9$ GeV/c^2 in this table. Values received for N_η and N_ω in these regions are in resonable agreement and result obtained

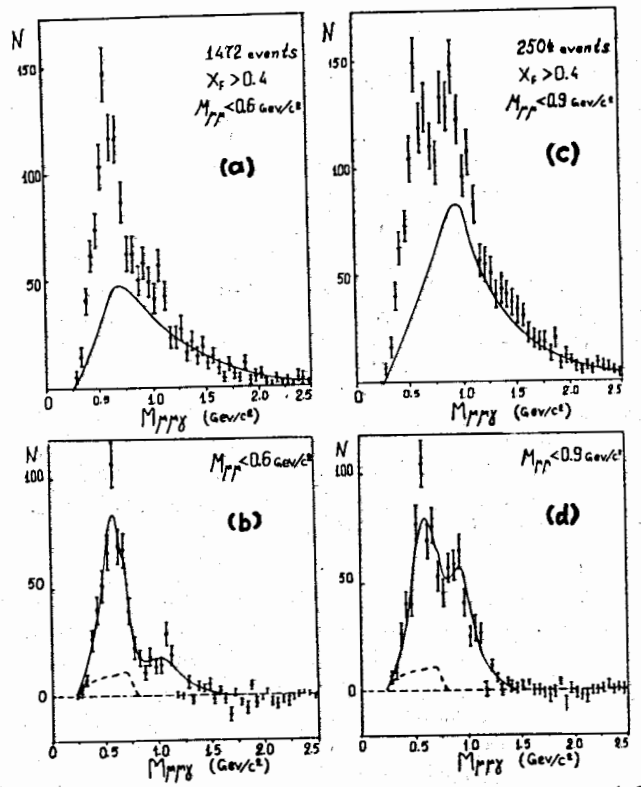

Fig.2. The $\mu^+\mu^-\gamma$ - invariant mass spectra: a) $M_{\mu\mu} < 0.6$ GeV/c², before subtracting random $\mu^+\mu^-\gamma$ - background from π^0 - decay (full line); b) $M_{\mu\mu} < 0.6$ GeV/c², after subtracting random $\mu^+\mu^-\gamma$ - background from π^0 - decay. Dashed curve shows the expected contribution from ω - decay. Full curve - result of the fitting procedure (see text); c), d) similar to (a), (b), but for $M_{\mu\mu} < 0.9$ GeV/c².

Table 1

The fitted resonance contributions to the $\mu\mu\gamma$ mass distribution

Mass	$M_{\mu\mu} < 0.6$ GeV/c²			$M_{\mu\mu} < 0.9$ GeV/c²	$M_{\mu\mu} < 0.6$ GeV/c²
Solution	I	II		II	II
a_{π^0} %	64±6	56±6	N_{π^0}	1734±150	828±88
a_η %	23±3	24±3	N_η	336±26	352±44
$a_{\eta'}$ %	6±2	10±2	$N_{\eta'}$	273±31	146±29
a_ω %	7±4	10^{+8}_{-5}	N_ω	161^{+80}_{-50}	146^{+117}_{-73}

for $N_{\eta'}$ is in a good accord with the measured transition formfactor of η' meson[33] (see below).

The acceptance for γ's in this experiment was studied by the Monte Carlo simulations. Secondary π^+ mesons accompanying $\mu^+\mu^-$ pairs were used as a source of π^0's in the interaction. This procedure was checked in the dimuon mass region $M_{\mu\mu} > 0.9$ GeV/c², where no contribution of any resonance is expected. The $\mu\mu\gamma$ mass and P_γ spectra are described by the simulated events very well. Overall normalization of the generated events to experimental one's provided the value of a ratio $\langle n_{\pi^0} \rangle / \langle n_{\pi^+} \rangle = 0.98 \pm 0.05$. The $F(M_{\mu\mu\gamma})$ distribution was evaluated on the assumption that π^+'s and $\mu^+\mu^-$ pair came from the same interaction and/or they were brought together randomly from different events (solution I and II in Table 1, respectively).

The evaluated $E(M_{\mu\mu\gamma})$ distribution for $\omega \to \pi^0 \mu\mu$ decay is shown in Figs 2b and 2d by the dashed curves. We have used the transition formfactor[31] $F_\omega(M^2_{\mu\mu}) = (1 - M^2_{\mu\mu}/\Lambda^2_\omega)^{-1}$; $\Lambda_\omega = 0.65 \pm 0.03$ GeV/c² in simulations of the virtual photon mass distribution.

In the last step of our analysis, the acceptance of γ's accompanying the detected $\mu^+\mu^-$ pair emitted from resonance decays was calculated. The obtained value of the acceptance of the η meson, $\epsilon_\gamma(x_F)$, as a function of a variable x_F of the registered $\mu^+\mu^-$ pair grows smoothly from 20% to 30% changing x_F from the threshold value 0.4 up to 1. For the $\eta'(\omega)$ meson, the γ acceptance was found to be 25% greater (30% less) than that for the η meson. The experimental formfactors $F_\eta(M^2_{\mu\mu}) = (1 - M^2_{\mu\mu}/\Lambda^2_\eta)^{-1}$ with $\Lambda_\eta = 0.72 \pm 0.09$ GeV/c² [32] and $|F_{\eta'}(M^2_{\mu\mu})|^2 = ((1 - M^2_{\mu\mu}/M^2_\rho)^2 + (\Gamma_\rho/M_\rho)^2)^{-1}$ [33] with $M_\rho = 0.77$ GeV/c² and $\Gamma_\rho = 0.15$ GeV/c² were taken into consideration. An important question, namely, to what extent acceptance depends on the assumptions about $d^2\sigma/dx_F dp^2_\perp$ of resonances was carefully investigated by the Monte Carlo simulations. Supposing the shape of $d^2\sigma/dx_F dp^2_\perp \sim (e^{-ax}F) * (e^{-bp^2_\perp})$, we have found that in a wide interval of the parameter values the acceptance is changed within ±5% around some reasonable value obtained with the following set of parameters: a = 3.3, b=4.4 (GeV/c)$^{-2}$ for η meson, a = 3, b = 2.5 (GeV/c)$^{-2}$ for ω meson and a = 2, b = 4 (GeV/c)$^{-2}$ for η' meson.

As a test, we have compared with experimental data the weighted sum of all calculated contributions to the γ momentum and the helicity angle distributions. (Helicity angle is defined as the one between the μ^+ direction and the opposite direction of the photon in the dimuon rest system). Full curves in Fig.3

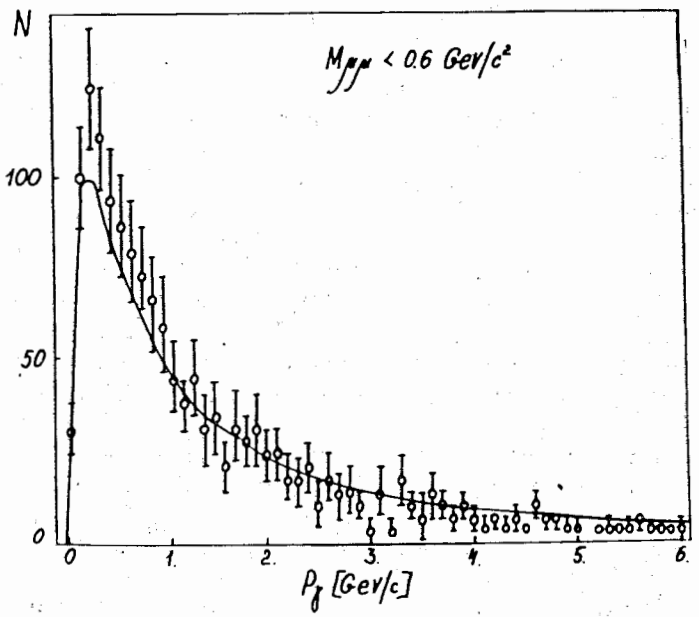

Fig.3. The momentum distribution of γ's accompanying $\mu^+\mu^-$ - pairs. Full line - result of the fitting procedure.

and Fig.4 correspond to the fitted values of parameters a_{π^0}, a_η, $a_{\eta'}$ and a_ω received for solution II (Table 1) and they describe the experimental distributions fairly well. One can recognize in Fig.4 that the experimental $\cos\theta_{\mu^+}$ distribution is somewhat broader than predicted by the π^0 background or ω decay. This observation supports the presence of the portion of η and η' mesons with angular dependence $\sim 1 + \cos^2\theta_{\mu^+}$.

The calculated acceptances for γ's allowed one to establish the final yields of dimuons from the resonance sources. The results are shown in Table 2. Both solutions lead us to the conclusion that resonance sources dominate in low mass dimuon production in the non-central region $x_F > 0.4$. As a meaningfull result, we took an average value of both solutions, i.e., Dalitz decay of η, η' and ω explained (92±7±10)% of all observed dimuons, where errors stand for statistical and systematical uncertainties, respectively. Systematical error is created mainly by inaccuracy in the radiation length determination of the converter (±5%) and by indefiniteness in scanning and measuring procedure of γ's.

The acceptance corrected x_F dependence of $\mu^+\mu^-$ pairs together with resonance contributions are shown in Fig.5a for the

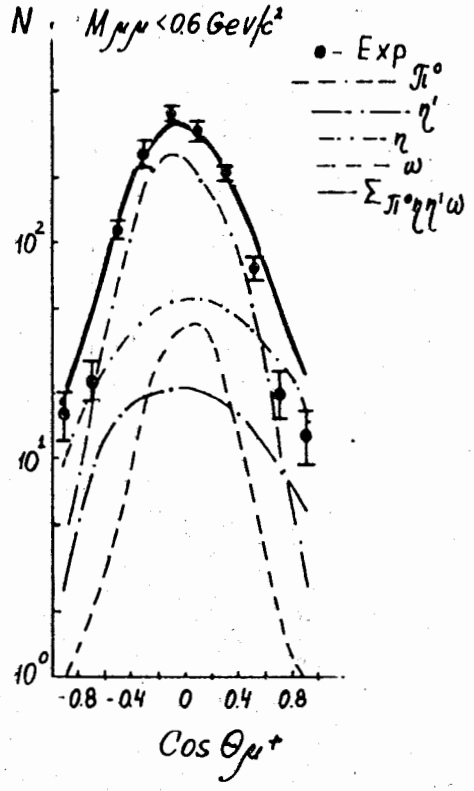

Fig.4. The helicity angle distribution ($\cos\theta_{\mu^+}$).

Table 2

The resonance contributions to the dimuon production

Mass	$M_{\mu\mu}$ < 0.6 GeV/c²	
Solution	I	II
p_η %	61±6	62±6
$p_{\eta'}$ %	10.5±2	17.5±3.5
p_ω %	13.7±8	19.4^{+12}_{-7}

low mass region ($0.2 < M_{\mu\mu} < 0.6$ GeV/c²) and, in Fig.5b for the ρ region ($0.6 < M_{\mu\mu} < 0.9$ GeV/c²). The similar distributions of $P_\perp^2$ dependences of $\mu^+\mu^-$ pairs are depicted in Fig.6. The resulting curves of Fig.5a and Fig.6a describe the data very well with an exception, perhaps, of the low $P_\perp^2$ region ($P_\perp^2 < 0.05$ (GeV/c)²). The x_F and $P_\perp^2$ distributions clearly exhibit greater steepness at low mass than in the ρ region suggesting the resonance pattern of dimuon production with masses below the ρ meson. The fit of an expression $(1-x_F)^a$ to the data provided values of $a = 1.88\pm0.07$ and $a = 0.97\pm0.05$ for the low mass and the ρ region, respectively. A behaviour of the $P_\perp^2$ spectrum appears rather complicated in shape and two exponential functions at least could approximate the distribution. As a rough approach one can use an exponential form $e^{-bP_\perp^2}$ with appropriate slopes $b_1 \sim 7.2$ (GeV/c)$^{-2}$ and $b_2 \sim 3.6$ (GeV/c)$^{-2}$ below and above $P_\perp^2 = 0.25$ (GeV/c)² (see Fig.6a). Again, this $P_\perp^2$ distribution is apparently much steeper than one in the ρ region (Fig.6b): $b_1 \sim 4.2$ (GeV/c)$^{-2}$ and $b_2 \sim 2.6$ (GeV/c)$^{-2}$.

Finally, the dimuon mass distribution is demonstrated in Fig.7a (thick histogram) with the $\mu^+\mu^-$ pair mass distributions arising from η, η' and ω Dalitz decays. The remaining mass spectrum after the subtraction of the resulting resonance contribution is depicted in Fig.7b. A lack of $\mu\mu$

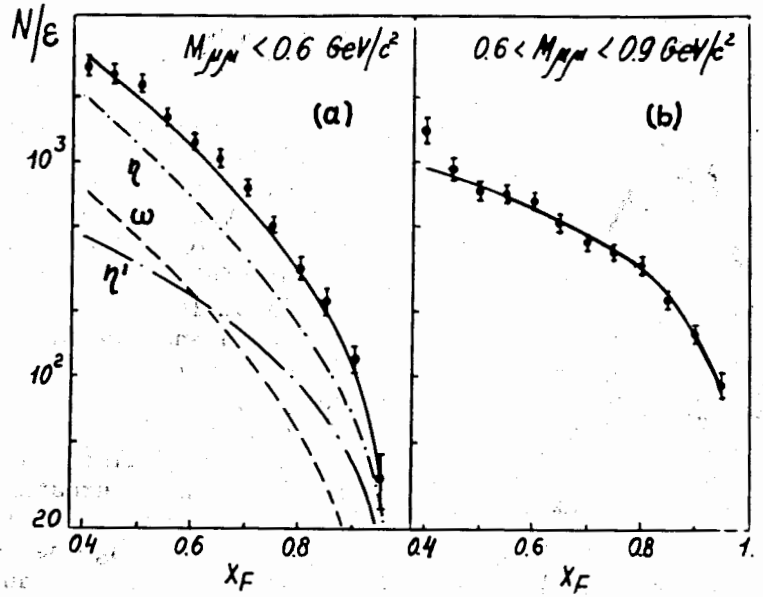

Fig.5. The acceptance corrected X_F distributions for $M_{\mu\mu} < 0.6$ GeV/c² (a) and for $0.6 < M_{\mu\mu} < 0.9$ GeV/c² (b).

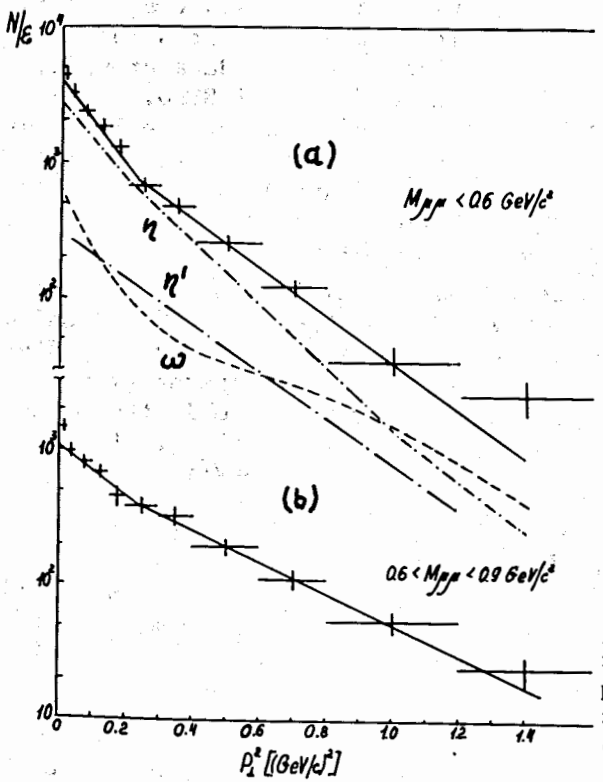

Fig.6. The acceptance corrected $P_\perp^2$ distributions for $M_{\mu\mu} < 0.6$ GeV/c² (a) and for $0.6 < M_{\mu\mu} < 0.9$ GeV/c² (b).

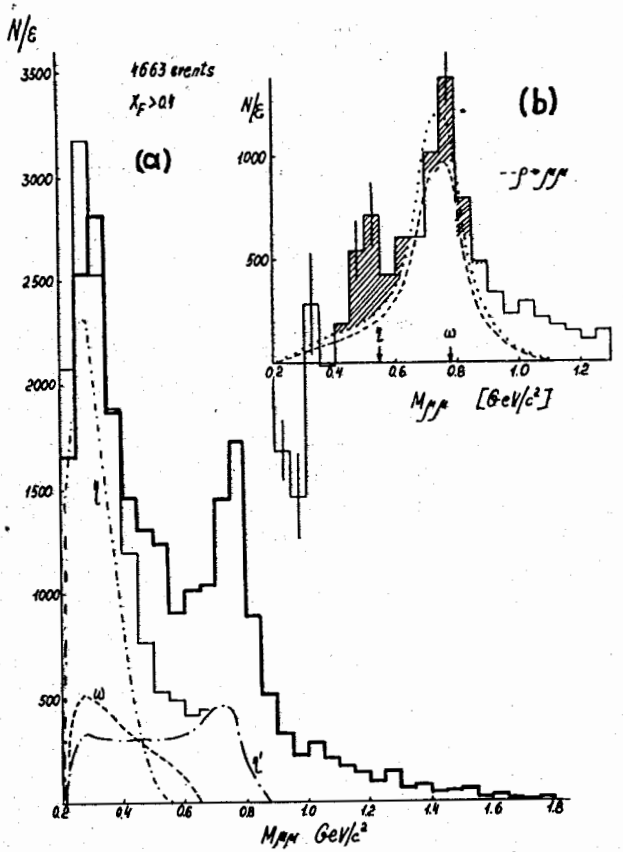

Fig.7. The invariant dimuon mass distributions corrected for acceptance: a) experimental histogram (thick line) and sum of contributions of η, η´and ω Dalitz decays (thin line); b) resulting experimental distribution after subtraction of Dalitz decay contributions of η, η´and ω.

events in the $M_{\mu\mu} < 0.3$ GeV/c² region has probably no physical meaning since this small effect would be explained by measuring losses of fast μ^- tracks. The dashed line in Fig.7b represents the Breit Wigner form of the ρ meson with the multiplicative factor $(M_\rho / M_{\mu\mu})^4$ taking into account the final photon propagator in an electromagnetic decay of $\rho \to \mu\mu$ [34]. Shaded area in Fig.7b would correspond to $\eta \to \mu\mu$ decay and $\omega \to \mu\mu$ decay. Possible ρ-ω interference effects are under study but their influence on the amount of η mesons registered is not important. Therefore, we can do an estimate of the ratio $BR(\eta \to \mu\mu)/BR(\eta \to \mu\mu\gamma)$ and it was found to be in reasonable agreement with the measured values in other experiments [32,35].

Thus, taking into account the $\eta \to \mu\mu$ decay and a tail of the $\rho \to \mu\mu$ decay one can conclude that (98±7±10)% of low mass dimuons are attributed to resonance decays. This result is in contradiction with conclusions of low statistic experiments[5-8] claiming that only 30% of dimuon production arise from the known sources and 70% of it remain unexplained even in the $x_F > 0.4$ region.

It is worth mentioning that the dimuon mass spectrum shown in Fig.7a has the same behaviour as the mass distribution of $\mu^+\mu^-$ pairs produced in the 225 GeV/c π^-C interactions with $x_F > 0.07$ [2,36] suggesting the nonexistence of any ($M_{\mu\mu}$, x_F) correlation in the whole measured mass interval ($0.2 < M_{\mu\mu} \leq 2$ GeV/c^2). Moreover, a form of the mass spectrum of direct dimuons observed at 225 GeV/c (~60% of all $\mu^+\mu^-$ pairs[4]) is the same as the resulting mass distribution of Dalitz pairs coming from η, η' and ω decays. Using various assumptions about the η and ω meson production authors of paper[4] concluded that in the $x_F \geq 0.5$ region the dimuons produced in the 225 GeV/c π^-C interactions could be attributed to resonance sources and, consequently, the cross section for continuum is 10 times smaller than it was found in low energy experiments[5-8].

The measured cross section $d\sigma/dx_F$ for the anomalous dilepton production at energies (5-18) GeV[3-8] has been approximated in the whole $x_F > 0.1$ region by an exponential form with slope of 6.3±0.1[4]. Similar dependence was also found at 225 GeV/c in the region $x_F \geq 0.07$, although in this case the residual x_F distribution is much steeper (slope is ~15.9[4]) and, therefore, the Feynman scaling is not obeyed.

The result of the present experiment settled this question and apparently prefers the very steep $d\sigma/dx_F$ cross section for continuum production. The soft annihilation model[18-21] described the behaviour of x_F, $P_\perp$ and $M_{\mu\mu}$ dependences obtained in the low energy π meson experiments fairly well and, therefore, the $d\sigma/dx_F \sim e^{-16x_F}$ is in contradiction with predictions of this model. Nevertheless, it seems to us that the final decision would be done after the comprehensive measurements of η, η' and ω cross section at 225 GeV/c.

We would like to thank Professors S.S.Gerstein, L.G.Landsberg, A.K.Likhoded, J.Pisut and A.Kalinovsky for stimulating discussions and criticism and T.Soukup, S.Valkar and A.Valkarova for their help at the initial stage of the experimental analysis.

REFERENCES

1. Anderson K.J. et al. - Phys. Rev.Lett., 1976, 37, p.799.
2. Branson J.B. et al. - Phys.Rev.Lett., 1977, 38, p.580; Henry G.G. - Ph.D. Thesis, University of Chicago, 1978 (unpublished).
3. Stroynowski R. et al. - Phys. Lett., 1980, 97B, p.315.
4. Blockus D. et al. - Nucl. Phys., 1982, B201, p.205.
5. Stekas J. et.al. - Phys.Rev.Lett., 1981, 47, p.1686.
6. Adams M.R. et al. - Phys. Rev., 1983, D27, p.1977.
7. Bunnell K. et al. - Phys.Rev.Lett., 1978, 40, p.136.
8. Haber B. et al. - Phys.Rev., 1980, D22, p.2107.
9. Mikamo S. et al. - Phys.Lett., 1981, 106B, p.428.
10. Morse W.M. et al. - Phys.Rev., 1978, D18, p.3145.
11. Grannan D.M. et al.- Phys.Rev., 1978, D18, p.3150.
12. Alspector J. et al. - Phys.Lett.,1979, 81B, p.397.
13. Dzhelyadin R.I. et al. - Nucl. Phys., 1981, B179, p.189.
14. Faessler M. et al. - Phys.Rev., 1978, D17, p.689.
15. Guy J. et al. - Phys.Lett., 1977, 66B, p.300.
16. Goshaw A.T. at al. - Phys.Rev., 1981, D24, p.2829.
17. Hedberg V. - Ph.D. Thesis, Lund University, LUNFD6/(NFFL-7037), 1987.
18. Bjorken J.D., Weisberg H. - Phys. Rev., 1976, D13, p.1405.
19. Cerny V. et al.- Acta.Phys.Pol., 1978, B9, p.901.
20. Cerny V. et al.- Acta. Phys.Pol., 1979, B10, p.537.
21. Cerny V. et.al. - Phys.Rev., 1981, D24, p.652.
22. Zakharov B.G. - Sov.J.Nucl.Phys., 1987, 46, p.674.
23. Goshaw A.T. et al. - Phys.Rev.Lett., 1979, 43, p.1065.
24. Chliapnikov P.V. et al. - Phys.Lett., 1984, 141B, p.276.
25. Schukraft J. - Recent results from HELIOS, preprint CERN-EP/88-176, to appear in Proc. 7th Int. Conf. on Ultrarelativistic Nucleus-Nucleus Collisions, Lenox, 1988.
26. Javrishvili A.K. et al. - Nucl. Instr. and Meth., 1980, 177, p.381; Vertogragov L.S. et al. - JINR Preprint P13-80-78,Dubna, 1980.
27. Bannikov A.V. et al. - Prib.Tekhn.Eksp., 1989, 2, p.69 (in Russian).
28. Böhm J. et al. - Prib.Tekhn.Eksp., 1981, 5, p.55 (in Russian).
29. Adam Gy. et al. - JINR Preprint 13-88-130, Dubna, 1988.
30. Todorova G. - Nucl.Instr and Meth., 1984, 227, p.335.
31. Dzhelyadin R.I. et al. - Phys.Lett., 1981, 102B, p.296.
32. Viktorov V.A. et al. - Sov. J. Nucl. Phys., 1980, 32, p.998.

33. Viktorov V.A. et al - Sov.J.Nucl. Phys., 1980, 32, p.1005.
34. Parson R.G., Weinstein R. - Phys.Rev.Lett., 1968, 20, p.1314.
35. Viktorov V.A. et al. - Sov.J.Nucl.Phys., 1980, 32, p.1002.
36. Stroynowski R. et al. - Phys.Rep., 1981, 71, p.1.

Received by Publishing Department
on June 28, 1989.